

Efficient Transfer Learning for Video-language Foundation Models

Haoxing Chen¹, Zizheng Huang^{1,2,3}, Yan Hong¹, Yanshuo Wang^{1,4}, Zhongcai Lyu¹,
Zhuoer Xu¹, Jun Lan¹, Zhangxuan Gu^{1*}

¹Tiansuan Lab, Ant Group, ²Nanjing Univeristy

³Shanghai Innovation Institute, ⁴Australian National University

hx.chen@hotmail.com

Abstract

Pre-trained vision-language models provide a robust foundation for efficient transfer learning across various downstream tasks. In the field of video action recognition, mainstream approaches often introduce additional modules to capture temporal information. Although the additional modules increase the capacity of model, enabling it to better capture video-specific inductive biases, existing methods typically introduce a substantial number of new parameters and are prone to catastrophic forgetting of previously acquired generalizable knowledge. In this paper, we propose a parameter-efficient Multi-modal Spatio-Temporal Adapter (MSTA) to enhance the alignment between textual and visual representations, achieving a balance between generalizable knowledge and task-specific adaptation. Furthermore, to mitigate over-fitting and enhance generalizability, we introduce a spatio-temporal description-guided consistency constraint. This constraint involves providing template inputs (e.g., "a video of {cls}") to the trainable language branch and LLM-generated spatio-temporal descriptions to the pre-trained language branch, enforcing output consistency between the branches. This approach reduces overfitting to downstream tasks and enhances the distinguishability of the trainable branch within the spatio-temporal semantic space. We evaluate the effectiveness of our approach across four tasks: zero-shot transfer, few-shot learning, base-to-novel generalization, and fully-supervised learning. Compared to many state-of-the-art methods, our MSTA achieves outstanding performance across all evaluations, while using only 2-7% of the trainable parameters in the original model.

1. Introduction

Multi-modal foundation models (e.g., CLIP [28], ViCLIP [36], BLIP2 [21]), trained on large-scale paired multi-

*Corresponding author. Code will be available at <https://github.com/chenhaoxing/ETL4Video>.

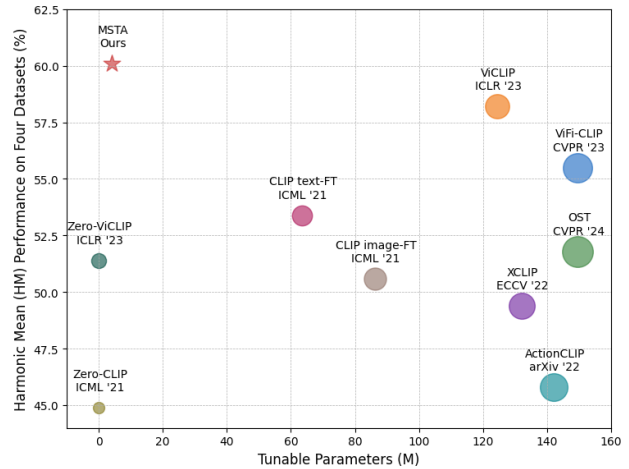


Figure 1. We compared the number of trainable parameters of our method with other state-of-the-art methods, as well as the average Harmonic Mean Performance on the base-to-novel generalization task across four datasets. It can be observed that our method uses fewer parameters while achieving state-of-the-art results.

modal datasets, have demonstrated exceptional generalization capabilities. The semantic visual concepts enabled by extensive multi-modal alignment can be effectively transferred to various downstream tasks, such as few-shot image/video classification [3, 19, 29, 43], open-vocabulary detection [12, 39], and segmentation [23]. In this paper, we focus on transferring the pre-trained multi-modal foundation models model (i.e., CLIP [28] and ViCLIP [36]) to video action recognition tasks, highlighting their significant potential to advance research in this domain.

The key to the adaptation process of foundational multi-modal models lies in injecting domain-specific expertise. In video action recognition, this need is particularly evident due to the dynamic and temporal nature of video data, requiring models to effectively capture context and temporal relationships. Consequently, existing methods typically enhance pre-trained CLIP models by integrating carefully

designed prompts [37], adapters [25, 41, 44], or temporal modules [24] to better acquire video-specific knowledge. For instance, XCLIP [24] employs cross-frame attention and multi-frame integration modules to model temporal information. ActionCLIP [34] uses pre-training to generate robust representations, applying prompt engineering to align the action recognition task closely with the pre-trained model, followed by fine-tuning to achieve superior performance. Despite the increased model capacity resulting from numerous learnable parameters, such approaches can lead to catastrophic forgetting, thereby diminishing the generalizability of the original models.

Alternatively, Wang *et al.* [36] proposed ViCLIP to enhance CLIP performance specifically for video understanding. ViCLIP is trained on extensive video-text pairs and incorporates spatiotemporal attention within the visual encoder, retaining other CLIP components unchanged. However, current research has not yet explored effective transfer learning methods specifically designed for ViCLIP, and existing CLIP-based methods cannot be directly applied.

Thus, the critical question arises: *Is there an efficient fine-tuning method for pre-trained models that preserves generalizability?* One possible approach is directly applying efficient transfer methods used for image/text foundation models, such as LoRA [17] and AdaptFormer [5], to video tasks. However, these methods primarily rely on uni-modal information, making them unsuitable for multi-modal models. Another simple strategy involves independently applying adapters to each modality, but this overlooks the interrelation between text and video representations. Consequently, directly applying identical adapters may not effectively capture task-specific nuances that vary across vision and language modalities. Furthermore, existing approaches do not fully address the distinct characteristics inherent in text and video representations. Effective transfer learning typically involves balancing discrimination and generalization—fine-tuning task-specific discriminative features while preserving features broadly applicable across different tasks.

To this end, we propose a novel Multi-modal Spatio-Temporal Adapter (MSTA) architecture for multi-modal foundation models such that the text and video representations can be better aligned. As shown in Fig. 1, our method achieves the best generalization performance with a minimal number of parameters. Specifically, our MSTa includes independent projection layers for the text and video branches to learn task-specific knowledge for each modality. To achieve effective alignment between modalities, we introduce a shared unified feature projection layer, which is jointly utilized by both modalities. During the fine-tuning phase, this shared feature space can receive gradients from both modalities [40], thereby optimizing the alignment between them. For the video branch, we further design two simple up-projection layers to enhance the adaptation capa-

bilities for temporal and spatial features. To further mitigate over-fitting and enhance the generalizability, we introduce a spatio-temporal description-guided consistency constraint. This method successfully transfers knowledge from a frozen encoder to a learnable encoder through knowledge distillation, allowing the model to maintain the generalization strength of the pre-trained base model when handling new tasks in few-shot scenarios [30]. Specifically, we impose a consistency constraint on the text branch between the trainable model with MSTa and the pre-trained model. We leverage a pre-trained large language model (e.g., DeepSeek [7]) to generate more detailed and descriptive sentences of temporal and spatial features, and impose a consistency constraint between the representations of the learnable text encoder and the pre-trained text encoder based on these sentences. To validate the effectiveness of our model, we perform extensive experiments across six benchmark datasets: Kinetics-400 [1], Kinetics-600 [2], UCF-101 [31], HMDB-51 [20], SomethingSomething V2 [13], and ActivityNet [15]. The results show that our approach attains state-of-the-art performance in open-vocabulary tasks, such as zero-shot and few-shot learning, and consistently enhances performance when integrated with existing pipelines in fully supervised settings.

The key contributions of this work are as follows:

- We propose a novel Multi-modal Spatio-Temporal Adapter (MSTA) that contains separate projection layers to improve feature representations for video and text encoders independently. Additionally, we implement a shared projection layer to improve the alignment between video and language representations.
- We propose a spatio-temporal description-guided consistency constraint for large multi-modal foundation models, enabling them to learn new tasks from a small number of samples while maintaining their generalization capability.
- Extensive experiments demonstrate that MSTa achieves an optimal balance between new and old knowledge while training only a small number of parameters. Comprehensive ablation studies showcase the scalability and effectiveness of our proposed method.

2. Related Works

Multi-modal Foundation Models. The latest advances in multi-modal foundation models have significantly impacted the field of computer vision, especially in tasks that combine language and vision. Representative models include, but are not limited to, CLIP [28], BLIP [21], Florence [42], Kosmos [26], InternVideo [35], and ViCLIP [36]. These models leverage self-supervised paradigms extracted from large-scale multi-modal web data for training. For example, CLIP [28] is trained using contrastive loss [33] on approximately 400 million image-text pairs, while ViCLIP [36] is trained on about 10 million video-text pairs. By collecting

more multi-modal data, these models have demonstrated promising performance across various downstream applications. Despite their ability to learn generalized representations, effectively adapting these pre-trained models to specific downstream tasks remains a major challenge, particularly in few-shot settings. To address this, many studies have proposed various methods tailored to different tasks, such as few-shot action recognition [29, 34], video question answering [11], and segmentation [9]. In contrast, this work proposes a novel multi-modal spatio-temporal adapter to effectively adapt multi-modal foundation models for generalization tasks.

Efficient Transfer Learning. Traditional approaches [8, 10] migrate models to downstream tasks by fine-tuning all parameters of the pre-trained network. However, as model sizes increase, this traditional paradigm faces a significant computational burden, and fine-tuning a large number of parameters often leads to severe overfitting, especially in low-sample scenarios. Recently, numerous methods [3, 19, 29, 43] have been proposed to explore the adaptation of pre-trained vision-language models [28, 36] to downstream tasks. In this paper, we focus on transferring pre-trained models to video understanding tasks. ViFi-CLIP [29] demonstrates that direct fine-tuning exhibits good generalization capabilities across various settings. Open-VCLIP [38] constructs an open-vocabulary video model by interpolating the model weights and its optimization trajectory. Vita-CLIP [37] uses multi-level prompts to extract discriminative information. X-CLIP [24] introduces cross-frame attention and multi-frame integration modules for temporal modeling. OST [6] optimizes text knowledge by leveraging large language models to generate spatio-temporal descriptors, and proposes an optimal descriptor solver to enhance generalization. MoTE [44] inserts a mixture-of-temporal-experts into the visual encoder to capture diverse views of data bias. However, all of these methods require learning a large number of parameters and suffer from catastrophic forgetting of the original generalizable knowledge. Moreover, these methods are specifically designed for CLIP [28], making them unsuitable for the latest base model, i.e., ViCLIP [36]. ViCLIP is a pre-trained model based on CLIP, trained on 10 million video-text pairs. Our work addresses these challenges by designing an efficient transfer learning approach tailored for ViCLIP, demonstrating superior results across various settings.

3. Methods

3.1. Preliminaries

We adopt ViCLIP [36] as the pre-trained video-language foundation model in our method. ViCLIP is an improved version of CLIP that replaces the native attention in the visual encoder with spatiotemporal attention, while keeping other design components unchanged. It uses pre-trained

CLIP weights for initialization. The model is trained on the InternVid-10M dataset [36], with the optimization objective being the contrastive loss between input video and text embeddings. ViCLIP is composed of two branches: a text branch with encoder E_t and a vision branch with encoder E_v . These two branches enable it to understand and bridge the semantic gap between textual descriptions and visual content. In particular, a video $V \in \mathbb{R}^{T \times H \times W \times 3}$ will be fed into the encoder E_v to obtain the video feature x as follows:

$$x_0 = \text{PatchEmbed}(V), \quad (1)$$

$$[c_i, x_i] = \mathcal{E}_v^i([c_{i-1}, x_{i-1}]), i = 1, 2, \dots, L, \quad (2)$$

$$x = \text{PatchProj}(c_L). \quad (3)$$

Here, PatchEmbed first divides the input video V into fixed-size patches, projecting them into feature embeddings. A learnable class token c_0 is then concatenated with these embeddings, forming $[c_0, x_0]$, which is subsequently passed through L transformer blocks, represented as $\{\mathcal{E}_v^i\}_{i=1}^L$. Finally, the class token c_L from the last transformer block \mathcal{E}_v^L is projected into the video feature x via a projection layer PatchProj, positioning the feature in the shared vision-language space. In a similar manner, a text description T is processed through the text encoder E_t to obtain the text feature w as follows:

$$w_0 = \text{TextEmbed}(T), \quad (4)$$

$$w_i = \mathcal{E}_t^i(w_{i-1}), i = 1, 2, \dots, L, \quad (5)$$

$$w = \text{TextProj}(w_L). \quad (6)$$

As shown, this process involves three steps: first, TextEmbed is used to tokenize and project the input text description into the initial word embedding w_0 . Next, a series of transformer blocks $\{\mathcal{E}_t^i\}_{i=1}^L$ progressively abstracts the features, producing a refined embedding w_L at the final layer. Finally, TextProj projects the output w_L from the last transformer block \mathcal{E}_t^L into the common vision-language space. Given these features, we compute the cosine similarity scores $\text{sim}(x, w)$ between the video and text descriptions across different domains or tasks to perform task-specific predictions.

3.2. Multi-modal Spatio-Temporal Adapter

Our work mainly focuses on generalization tasks (i.e., few-shot generalization [19, 43] and zero-shot generalization [34]), where the pre-trained multi-modal foundation models are first fine-tuned on a limited set of training samples, and then applied to recognize unseen instances. For such problems, a good instance representation should not only be discriminative but also exhibit strong generalization capabilities across different types of datasets. Typically, adding additional parameters helps better fit the training data distribution, thereby improving performance on seen

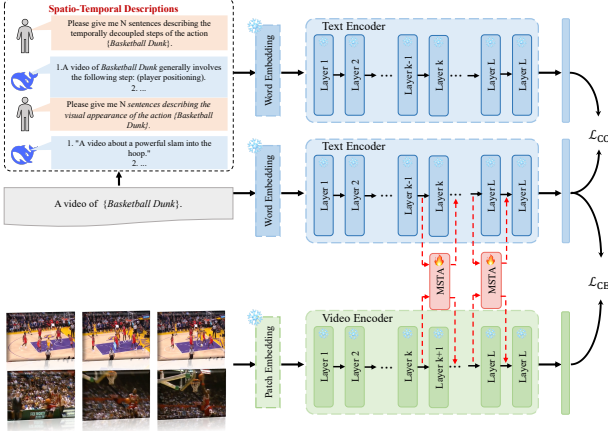


Figure 2. The proposed Multi-modal Spatio-Temporal Adapter (MSTA) is designed for transformer-based multi-modal foundation models. It optimizes only the additional adapters, keeping the pretrained CLIP model frozen. To balance discrimination and generalization, we selectively fine-tune a few higher layers ($\geq k$). MSTAs employ shared weights for video and text representations, enabling the model to capture shared cues from both modalities.

tasks. However, models optimized for specific target distributions are often highly sensitive to external distribution shifts, which may lead to poor generalization performance in downstream tasks involving unknown video categories. While, in theory, expanding the training dataset to cover more unseen categories could mitigate this issue, the high computational and data acquisition costs associated with video data make this approach impractical. Therefore, it is crucial to develop a foundational model architecture with enhanced generalization capability.

Recently, parameter efficient fine tuning [5, 17] (PEFT) has proven to be an effective method for transfer learning in large models. Two representative approaches are LoRA [17] and AdaptFormer [5]. However, these methods are designed for uni-modal models and cannot be directly applied to multi-modal models. While it is possible to apply adapters separately to the two modalities, the lack of interaction between visual and textual information limits their performance. Therefore, we propose a new adapter-based efficient transfer learning framework as described below.

Holistic design. As illustrated in Fig. 2, unlike most existing methods that introduce adapters or tokens across the entire network or into lower layers, our adapter \mathcal{A} is selectively incorporated into only a few higher layers of both the video and text encoders. Specifically, for the video encoder E_v , we incorporate adapters $\{\mathcal{A}_v^j\}_{j=k}^L$ starting from the k -th transformer block, modifying Eq. (2) as follows:

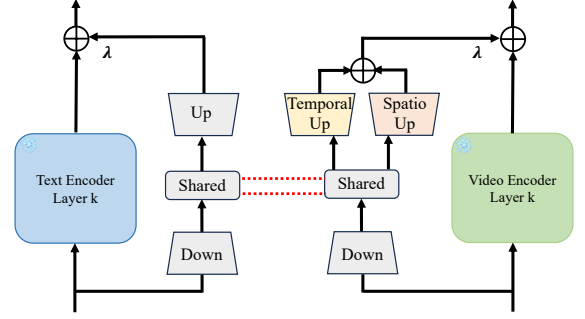


Figure 3. Overview of the proposed Multi-modal Spatio-Temporal Adapter (MSTA).

$$[c_i, x_i] = \mathcal{E}_v^i([c_{i-1}, x_{i-1}]), \quad i = 1, 2, \dots, k-1, \quad (7)$$

$$[c_j, x_j] = \mathcal{E}_v^j([c_{j-1}, x_{j-1}]) + \lambda \boxed{\mathcal{A}_v^j([c_{j-1}, x_{j-1}])}, \quad j = k, k+1, \dots, L. \quad (8)$$

Here, the portion inside the box represents the trainable blocks. The coefficient λ is used to balance task-specific knowledge with general pre-trained knowledge. Notably, setting $\lambda = 0$ reduces the model to the original transformer block, without incorporating any additional knowledge. Similarly, we add adapters $\{\mathcal{A}_t^j\}_{j=k}^L$ to the text encoder E_t and modified Eq. (5) as follows:

$$w_i = \mathcal{E}_t^i(w_{i-1}), \quad i = 1, 2, \dots, k-1, \quad (9)$$

$$w_j = \mathcal{E}_t^j(w_{j-1}) + \lambda \boxed{\mathcal{A}_t^j(w_{j-1})}, \quad j = k, k+1, \dots, L. \quad (10)$$

Specific design. According to [16], the adapters in both the text branch and the video branch consist of down-projection layers (encoders), adapter layers, and up-projection layers (decoders). As shown in Fig. 3, to bridge the representations in both branches and reduce the semantic gap, we do not independently adapt the adapters in the video and text branches. Instead, we aggregate these bi-modal signals through a shared projection layer. During fine-tuning, this shared feature space receives gradients from both modalities, thereby optimizing their alignment. Additionally, for the video branch, we designed two types of up-projection layers: one spatial up-projection layer and one temporal up-projection layer, to further enhance the adaptability to spatiotemporal features. Formally, this process can be summarized as follows:

$$\mathcal{A}_v^k(h_k) = \mathbf{W}_v^{ku-s} \cdot h_k + \mathbf{W}_v^{ku-t} \cdot h_k, \quad (11)$$

$$h_k = \sigma(\mathbf{W}_v^{ks} \cdot \sigma(\mathbf{W}_v^{kd} \cdot [c_k, x_k])). \quad (12)$$

A similar process is added to text encoder as follows:

$$\mathcal{A}_t^k(w_k) = \mathbf{W}_t^{ku} \cdot \sigma(\mathbf{W}_t^{ks} \cdot \sigma(\mathbf{W}_t^{kd} \cdot w_k)). \quad (13)$$

Here, \mathbf{W}^{ku} and \mathbf{W}^{kd} represent the "Up" and "Down" projection layers of the k -th layer, as illustrated in Fig. 3, with the modality branch indicated by the subscripts. \mathbf{W}_v^{ku-s} is the spatial up-projection layer implemented by a linear layer, while \mathbf{W}_v^{ku-t} is the temporal up-projection layer implemented by a 3D convolution layer. \mathbf{W}^{ks} denotes the k -th projection layer, which is shared across different branches.

3.3. Spatio-Temporal Description-guided Consistency Constraint

To address the issue of decreased generalization ability due to over-fitting on downstream tasks, we propose the Spatio-Temporal Description-guided Consistency constraint. This constraint ensures that the embeddings generated by the trainable model (adjustable adapter parameters in the image and text branches) do not significantly deviate from those generated by the pre-trained multi-modal foundation model, while enhancing the understanding of temporal and spatial features. In the language branch, we leverage a pre-trained large language model (LLM) [7] to generate more descriptive sentences that better capture the temporal and spatio aspects of actions. The spatio description aims to capture static visual elements that can be discerned from a single image, such as scenes and common objects. The temporal description, on the other hand, is designed to decompose action categories in a step-by-step manner, describing the temporal evolution of actions. To generate spatio descriptions, we use the following prompt with category name $\{\mathbf{cls}\}$ to query LLM: "Please give me N sentences describing the visual appearance of the action $\{\mathbf{cls}\}$ ". For temporal descriptions, we utilize the the following temporal prompt: "Please give me N sentences describing the temporally decoupled steps of the action $\{\mathbf{cls}\}$ ". Through the above operations, we obtain the spatio descriptions DES_s and temporal DES_t , each containing N descriptions.

Subsequently, we feed sentences based on standard template (i.e., a video of $\{\mathbf{cls}\}$.) into the learnable branch, while spatio/temporal descriptions are provided to the pre-trained branch. We employ cosine distance as a consistency constraint between the embeddings from the pre-trained branch and the learnable branch. The pre-trained encoder extracts features from the spatio/temporal descriptions, allowing the consistency constraint to be defined as:

$$\mathcal{L}_{CC} = 2 - \frac{w^c \cdot D_s^c}{\|w^c \cdot D_t^c\| \|D_s^c\|} - \frac{w^c}{\|w^c\| \|D_t^c\|}, \quad (14)$$

where w^c indicates the text embedding for class c of the pre-trained branch, and D_s^c represents the mean embedding of the spatio descriptions for class c , obtained by averaging the features of the input descriptions processed through the pre-trained branch. Similarly, D_t^c is computed for the temporal descriptions. This consistency constraint loss is combined with a supervised loss to create the final loss function. The

Table 1. Implementation details of MSTA

Dataset	Batch size	Learning rate	Training epochs	α	λ	Dims	N	Dropout	Layers
Base-to-novel generalization									
K-400	32	1.e-03	11	1.0	0.005	256	2	0.1	1-12
SSv2	32	1.e-03	11	1.0	0.005	256	2	0.1	1-12
HMDB-51	32	1.e-03	11	1.0	0.005	256	2	0.1	1-12
UCF-101	32	1.e-03	11	1.0	0.005	256	2	0.1	1-12
Few-shot learning									
SSv2	32	1.e-03	50	1.0	0.005	128	2	0.1	8-12
HMDB-51	32	1.e-03	50	1.0	0.005	128	2	0.1	8-12
UCF-101	32	1.e-03	50	1.0	0.005	128	2	0.1	8-12
Zero-shot Transfer									
K-400	256	8.e-03	100	1.0	0.001	128	2	0.1	1-12
Few-shot learning									
K-400	256	8.e-03	100	1.0	0.001	128	2	0.1	1-12

supervised loss is given by:

$$\mathcal{L}_{CE} = -\log \frac{\exp(\text{sim}(x, w^c)/\tau)}{\sum_{k=1}^C \exp(\text{sim}(x, w^k)/\tau)}, \quad (15)$$

where τ is a temperature parameter controlling the sharpness of similarity scores. By combining these losses with a weighting factor α , the final loss function for MSTA becomes:

$$\mathcal{L} = \mathcal{L}_{CE} + \alpha \mathcal{L}_{CC}. \quad (16)$$

4. Experiments

4.1. Experimental Setup

Dataset. We conducted experiments on six video benchmarks: Kinetics-400 [1], Kinetics-600 [2], UCF-101 [31], HMDB-51 [20], and SomethingSomething V2 [13]. Our study covers multiple settings, including zero-shot transfer, few-shot learning, base-to-novel generalization and fully-supervised video recognition.

Architecture. We employ the ViCLIP [36] pre-trained ViT-B/16 in our experiments. For the zero-shot transfer, few-shot learning, base-to-novel generalization and fully-supervised settings, we incorporated our multi-modal spatio-temporal adapter starting from the 1st, 8th, 1st, and 1st transformer blocks and extended it to the last block in both the language and vision components.

Implementation Details. Table 1 outlines the implementation specifics for efficient transfer video recognition. All modules in MSTA are initialized using kaiming initialization [14]. We use AdamW [22] as the optimizer, with a weight decay of 0.001 and Adam’s β_1, β_2 set to 0.9 and 0.98, respectively. The linear warm-up consists of 5 epochs. For data augmentation during training, we apply ColorJitter (P=0.8), GrayScale (P=0.2), RandomResizedCrop, and FLIP (flip ratio=0.5). All experiments are conducted on 8 Nvidia Tesla-A100-80G GPUs.

Evaluation Protocols. (1) Zero-shot: Following previous works [6, 24], we evaluate zero-shot performance on UCF-101 [31], HMDB-51 [20], Kinetics-600 [2]. In zero-shot setting, we test using single view with 8 frames. (2) Few-shot

Table 2. Base-to-novel generalization: We compare the generalization ability of MSTA with models that adapt ViCLIP for video tasks. “HM” is the harmonic mean of base and novel accuracy, providing the trade-off between adaption and generalization. ”Zero-ViCLIP” refers to zero-shot ViCLIP, which directly uses the pre-trained ViCLIP for inference.

Method	GFLOPs	K-400			HMDB-51			UCF-101			SSv2		
		Base	Novel	HM									
Zero-shot pre-trained models													
Vanilla CLIP _(ICML'21)	281	55.1	55.2	55.1	50.6	48.1	49.3	78.0	63.8	70.2	4.8	5.4	5.1
Adapting pre-trained models													
ActionCLIP _(arXiv'22)	282	61.5	47.2	53.4	69.3	38.3	49.3	90.5	58.7	71.2	13.5	10.4	11.7
XCLIP _(ECCV'22)	145	74.7	56.7	64.5	69.9	45.3	55.0	90.7	59.5	71.9	8.9	6.8	7.7
A5 _(ECCV'22)	284	69.9	38.4	49.6	46.9	16.5	24.4	90.9	40.8	56.3	8.6	6.4	7.3
Tuning pre-trained models													
Vanilla CLIP _(ICML'21)	281	76.4	63.0	69.1	71.5	55.3	62.4	92.3	67.9	78.2	13.2	10.8	11.9
ViFi-CLIP _(CVPR'23)	281	76.8	61.3	68.2	74.5	53.9	62.5	92.5	68.5	78.7	16.5	12.4	14.2
OST _(CVPR'24)	-	75.4	59.6	66.6	75.1	34.4	47.2	96.1	68.9	80.3	15.3	11.5	13.1
ViCLIP _(ICLR'23)	161	78.5	65.3	71.3	77.9	52.4	62.7	95.1	71.5	81.6	19.4	15.2	17.0
Efficient transfer pre-trained models													
Zero-ViCLIP _(ICLR'23)	161.74	68.7	63.4	65.9	62.5	48.9	54.9	81.7	69.8	75.3	9.3	8.9	9.1
+ AdaptFormer _(NeurIPS'22)	179.80	77.7	65.6	71.1	77.5	54.9	64.3	94.9	72.7	82.3	20.4	14.6	17.0
+ LoRA _(NeurIPS'22)	179.80	77.6	65.3	70.9	<u>77.2</u>	54.6	64.0	95.1	72.3	82.1	19.5	13.6	16.0
+ MSTA	179.84	78.2	<u>66.2</u>	<u>71.7</u>	<u>77.2</u>	<u>57.5</u>	<u>65.9</u>	<u>95.6</u>	<u>72.8</u>	<u>82.7</u>	<u>21.9</u>	<u>16.3</u>	<u>18.7</u>
+ MSTA + \mathcal{L}_{CC}	179.84	78.5	66.5	72.0	77.5	57.9	66.3	<u>96.0</u>	72.9	82.9	22.2	16.5	18.9

Table 3. Comparisons with state-of-the-art methods for few-shot video recognition on HMDB51, UCF101 and Something-Something V2. We scaled up the task to categorize all categories in the dataset with only a few samples per category for training. Here K denotes training samples for each class. We report Top-1 accuracy using multi-view inference.

Method	GFLOPs	HMDB-51				UCF-101				SSv2			
		$K=2$	$K=4$	$K=8$	$K=16$	$K=2$	$K=4$	$K=8$	$K=16$	$K=2$	$K=4$	$K=8$	$K=16$
Zero-shot pre-trained models													
Vanilla CLIP _(ICML'21)	281	37.2	37.2	37.2	37.2	62.8	62.8	62.8	62.8	2.8	2.8	2.8	2.8
Adapting pre-trained models													
XCLIP _(ECCV'22)	145	53.5	57.8	62.9	64.5	49.3	76.2	84.1	91.6	4.4	5.2	6.6	11.1
A5 _(ECCV'22)	284	41.2	51.3	56.5	62.7	71.7	80.3	85.9	90.3	4.5	5.3	6.3	9.9
Tuning pre-trained models													
Vanilla CLIP _(ICML'21)	282	57.8	61.2	65.6	66.7	81.8	86.3	90.1	92.5	6.7	7.3	9.0	12.2
ViFi-CLIP _(CVPR'23)	281	57.5	<u>62.9</u>	64.7	66.6	80.5	85.3	90.2	93.2	6.5	7.7	8.3	12.9
OST _(CVPR'24)	-	60.0	62.5	65.6	67.3	83.0	88.4	91.3	<u>93.9</u>	7.3	8.4	8.5	11.5
MoTE _(NeurIPS'24)	141	<u>61.0</u>	63.7	<u>66.9</u>	68.5	88.1	90.7	92.2	93.7	7.4	8.7	9.8	12.5
ViCLIP _(ICLR'23)	161	53.7	60.4	<u>64.5</u>	<u>70.3</u>	83.0	88.0	92.1	93.2	8.7	9.7	11.6	15.4
Efficient transfer pre-trained models													
Zero-ViCLIP _(ICLR'23)	161	47.8	47.8	47.8	47.8	71.0	71.0	71.0	71.0	5.1	5.1	5.1	5.1
+ AdaptFormer _(NeurIPS'22)	179.80	60.0	61.8	66.6	70.1	84.8	88.7	91.7	93.3	8.5	10.1	11.5	15.2
+ LoRA _(NeurIPS'22)	179.80	59.4	61.4	66.5	69.4	83.5	88.3	90.9	92.7	8.4	9.5	11.1	14.9
+ MSTA	179.84	60.1	62.2	66.8	69.9	85.1	89.0	<u>92.3</u>	93.5	<u>9.0</u>	<u>10.1</u>	<u>12.7</u>	<u>16.6</u>
+ MSTA + \mathcal{L}_{CC}	179.84	61.2	62.3	67.1	70.4	<u>86.1</u>	<u>90.2</u>	92.7	94.8	9.1	10.4	13.4	17.5

and base-to-novel generalization: We evaluate on Kinetics-400 [1], UCF-101 [31], HMDB-51 [20], and Something-Something V2 [13]. Following [32], we adopt a multi-view for evaluation. (3) Fully-supervised: We evaluate the fully-supervised performance on Kinetics-400 [1], using 4 clips with 3 crops (i.e. 4×3 views) per video [24]. Each view

contains 8 sparsely sampled frames.

Baseline models. We compare our approach to efficient transfer learning methods [4, 6, 18, 24, 27, 29, 37, 44] that based on CLIP for video tasks. Since these methods are specifically designed for CLIP, they cannot be directly applied to ViCLIP. Therefore, we employed common

Table 4. Comparisons with state-of-the-art methods for zero-shot video recognition on HMDB51, UCF101 and Kinetics-600. We report Top-1 and Top-5 accuracy using single-view inference.

Method	Frames	HMDB-51	UCF-101	K600
Zero-shot pre-trained models				
ER-ZSAR _(ICCV'21)	16	35.3 ± 4.6	51.8 ± 2.9	42.1 ± 1.4
JigsawNet _(ECCV'22)	16	38.7 ± 3.7	56.0 ± 3.1	-
Adapting pre-trained models				
Vanilla CLIP _(ICML'21)	32	40.8 ± 0.3	63.2 ± 0.2	59.8 ± 0.3
XCLIP _(ECCV'22)	32	44.6 ± 5.2	72.0 ± 2.3	65.2 ± 0.4
A5 _(ECCV'22)	8 / 32	44.3 ± 2.2	69.3 ± 4.2	55.8 ± 0.7
Vita-CLIP _(CVPR'23)	32	48.6 ± 0.6	75.0 ± 0.6	67.4 ± 0.5
Tuning pre-trained models				
ViFi-CLIP _(CVPR'23)	32	51.3 ± 0.7	76.8 ± 0.8	71.2 ± 1.0
OST _(CVPR'24)	8	54.9 ± 1.1	77.9 ± 1.3	73.9 ± 0.8
ViCLIP _(ICLR'23)	8	51.9 ± 0.7	77.1 ± 0.9	71.5 ± 1.1
Efficient transfer pre-trained models				
Zero-ViCLIP _(ICLR'23)	8	39.8 ± 0.9	62.6 ± 0.5	59.2 ± 0.4
+ AdaptFormer _(NeurIPS'22)	8	54.1 ± 0.9	77.2 ± 0.6	72.8 ± 0.8
+ LoRA _(NeurIPS'22)	8	54.2 ± 0.5	77.3 ± 0.8	73.8 ± 0.7
+MSTA	8	55.3 ± 0.7	77.8 ± 0.9	74.1 ± 0.7
+MSTA+ \mathcal{L}_{CC}	8	55.8 ± 0.8	78.7 ± 0.9	74.5 ± 0.5

parameter-efficient fine-tuning methods [5, 16, 17] on ViCLIP to enable a more comprehensive comparison.

4.2. Main Results

Base-to-novel generalization. In Table 2, we compare our method with the state-of-the-art results under the base-to-novel setting. Our method achieves new state-of-the-art results on all datasets. Compared to OST [6] and Action-CLIP [34], which model video-specific inductive biases through full fine-tuning, our approach provides better base accuracy with minimal design modifications and demonstrates a significant improvement in novelty accuracy. Our method achieves a better trade-off between base and novel accuracies across all datasets and obtains the overall best harmonic mean. Moreover, it shows enhanced capability in understanding scene dynamics, particularly on temporally challenging datasets like SSv2. Specifically, compared to OST, we improve the recognition accuracy of the novel category on SSv2 from 11.5 to 15.8 (an increase of 30 37%). Our method also outperforms classic PEFT approaches (i.e., AdaptFormer [5], LoRA [17]), validating the effectiveness of MSTA and consistency constraints in enhancing generalization capabilities.

Few-shot learning. In Table 3, we conducted a challenging full-shot few-shot video recognition task, which requires rapid adaptation to new categories with limited samples, demanding both specialization and generalization. Our approach achieved 9 out of 12 best performances across different sample settings for all datasets, demonstrating strong learning capability and transferability. Notably, compared to the second-best method, MoTE [44], we used only 10% of its parameter count (i.e., 8.7M vs. 88M).

Table 5. Comparisons with state-of-the-art methods for fully-supervised video recognition on Kinetics-400. We report Top-1 and Top-5 accuracy using single-view inference.

Method	Frames	Tunable Param	K-400	
			Top-1	Top-5
XCLIP _(ECCV'22)	8	132	82.3	95.8
Vita-CLIP _(CVPR'23)	8	39	80.5	95.9
OST _(CVPR'24)	8	149.6	82.0	95.8
ViCLIP _(ICLR'23)	8	124.3	79.9	95.1
+ AdaptFormer _(NeurIPS'22)	8	7.9	80.2	95.5
+ LoRA _(NeurIPS'22)	8	9.4	80.3	95.4
+ MSTA	8	8.7	81.6	95.8
+ MSTA+ \mathcal{L}_{CC}	8	8.7	82.2	96.2

Zero-shot transfer. We present our zero-shot video recognition results in Table 4 and compare our approach with current state-of-the-art methods. First, the model is fine-tuned on the Kinetics-400 dataset [1] and directly evaluated on downstream datasets to assess its generalization capability to unseen classes. As shown in the table, our method significantly outperforms the conventional uni-modal zero-shot video recognition pipeline [4, 27]. Furthermore, we compare our approach with methods [6, 18, 24, 37] that adapt the CLIP model for zero-shot recognition using Kinetics-400, as well as methods that fine-tune ViCLIP with classic PEFT approaches (e.g., AdaptFormer [5], LoRA [17]). We observe consistent improvements across all datasets compared to these methods.

Fully-supervised learning. We also conducted fully supervised experiments on the large-scale video benchmark dataset Kinetics-400 to validate the effectiveness of our method in supervised settings. As shown in Table 5, our method achieved the best performance. Specifically, our method outperforms Vita-CLIP [37] by approximately 2% on K400.

4.3. Ablation Studies

We conduct ablation studies on base-to-novel settings in Table 6 to investigate the learning capacity and generalizability of our model in different instantiations.

Component-wise analysis of MSTA. We began by examining the impact of various adapter configurations. Specifically, we compared the performance of uni-modal adapters, which are adapters applied exclusively to either the vision (V-) or language (L-) branch, against the performance of our full MSTA model, which incorporates adapters in both modalities. Our findings, as presented in Table 4a, clearly indicate that the uni-modal adapters are outperformed by the full MSTA model. This suggests that the integration of both visual and textual information is crucial for optimal performance. Moreover, we discovered that omitting the shared projection layers (w/o Shared Layers) results in a noticeable

Table 6. Ablation studies over 4 datasets used in base-to-novel generalization setting.

Model Variants	Base	Novel	HM	Dims	Base	Novel	HM	λ	Base	Novel	HM
Only L-Adapter	66.1	51.5	57.9	64	67.5	52.2	58.9	0.001	67.7	53.1	59.5
Only V-Adapter	65.7	51.7	57.9	128	68.2	53.1	59.7	0.005	68.6	53.5	60.1
w/o Shared Layers	68.0	52.9	59.5	256	68.6	53.5	60.1	0.01	68.5	52.9	59.7
Full	68.6	53.5	60.1	512	68.7	53.3	60.0	0.05	67.1	40.3	50.4

(a) Performance with Different Model Variants (b) Dimensions of Shared Layers (c) Scaling Factor

α	Base	Novel	HM	N	Base	Novel	HM	Layer	1→6	1→12	7→12	8→12	10→12
0.1	68.1	53.2	59.7	2	68.6	53.5	60.1	Base	67.4	68.6	68.1	68.7	65.9
1.0	68.6	53.5	60.1	4	68.8	53.0	59.9	Novel	52.9	53.5	53.0	53.1	51.9
5.0	68.5	53.0	59.8	8	68.6	52.9	59.7	HM	59.3	60.1	59.6	59.9	58.1

(d) Weighting Factor (e) Discription Number (f) MSTa inserted layers.

performance drop. When these shared layers are included, we observe an increase in the harmonic mean (HM) from 59.5 to 60.1 across the four datasets.

Dimension of the Shared Layer. The dimension of the shared layer in our MSTa determines the number of parameters required to extract relationships from the features of the two modalities. We conducted an ablation study by systematically varying the dimension of the shared layer to assess its impact. As shown in Table 6b, accuracy for base categories peaks as the intermediate dimension increases, while accuracy for novel categories saturates around 256. This may be due to larger dimensions introducing more trainable parameters, which increases the risk of over-fitting.

Scaling Factor λ . The scaling factor λ balances general and task-specific features in MSTa. As shown in Table 6c, we found $\lambda = 0.005$ achieves the best trade-off (HM) between base and novel categories. Larger values enhance base-category performance but reduce generalization, while smaller values limit adaptability.

Weighting Factor α . The weighting factor α , associated with the consistency constraint loss, is a critical hyperparameter affecting model performance. As demonstrated in Table 6d, varying α significantly impacts model accuracy, with optimal performance observed at $\alpha = 1.0$. Deviating from this optimal value, either by increasing or decreasing α , results in performance degradation. These observations highlight the necessity of precise tuning of the consistency constraint to achieve an effective balance between model adaptability and generalization.

Numbers of Descriptions. We investigate the influence of varying the number of descriptions in Table 6e. We conducted experiments with 2, 4, and 8 spatio-temporal descriptions. It can be observed that the performance is better when $N = 2$. This may be because as N increases, the hallucination problem of the LLM becomes more severe, resulting in a significant amount of noisy descriptions.

Variants of Adding MSTa. We investigate the impact of incorporating MSTa into various encoder layers, with the results summarized in Table 6f. The performance consistently improves as the number of MSTa layers increases. Additionally, for the same number of MSTa layers, placing them in higher encoder layers (farther from the input) yields superior results. For instance, integrating MSTa into layers 7 to 12 achieves an HM score 0.3 points higher than integrating it into layers 1 to 6, despite both configurations involving six MSTa layers. Importantly, inserting MSTa into layers 8 to 12 provides the best performance for base class tasks, highlighting its particular benefit in few-shot learning scenarios that demand rapid adaptation to novel categories.

5. Conclusion

In conclusion, this paper introduces a novel Multi-modal Spatio-Temporal Adapter (MSTa) designed for efficient transfer learning in video-language foundation models. The MSTa aims to enhance alignment between text and video representations, achieving an optimal balance between general knowledge and task-specific knowledge. The proposed method incorporates a spatio-temporal description-guided consistency constraint to reduce overfitting and improve generalization, particularly beneficial in scenarios with limited data. Extensive experiments conducted on diverse tasks demonstrate outstanding performance and state-of-the-art results, achieved with minimal trainable parameters. Comprehensive ablation studies further confirm the effectiveness and scalability of the proposed approach. Overall, our work significantly advances the field of video action recognition by offering an efficient transfer learning framework that maintains the generalizability of pre-trained models while effectively adapting them to specific downstream tasks.

References

- [1] João Carreira and Andrew Zisserman. Quo vadis, action recognition? A new model and the kinetics dataset. In *CVPR*, pages 4724–4733, 2017. [2](#), [5](#), [6](#), [7](#)
- [2] Joao Carreira, Eric Noland, Andras Banki-Horvath, Chloe Hillier, and Andrew Zisserman. A short note about kinetics600. *arXiv preprint arXiv:1808.01340*, 2018. [2](#), [5](#)
- [3] Haoxing Chen, Yaohui Li, Zizheng Huang, Yan Hong, Zhuoer Xu, Zhangxuan Gu, Jun Lan, Huijia Zhu, and Weiqiang Wang. Conditional prototype rectification prompt learning. *arXiv preprint arXiv:2404.09872*, 2024. [1](#), [3](#)
- [4] Shizhe Chen and Dong Huang. Elaborative rehearsal for zero-shot action recognition. In *ICCV*, pages 13618–13627, 2021. [6](#), [7](#)
- [5] Shoufa Chen, Chongjian Ge, Zhan Tong, Jiangliu Wang, Yibing Song, Jue Wang, and Ping Luo. Adaptformer: Adapting vision transformers for scalable visual recognition. In *NeurIPS*, 2022. [2](#), [4](#), [7](#)
- [6] Tom Tongjia Chen, Hongshan Yu, Zhengeng Yang, Zechuan Li, Wei Sun, and Chen Chen. OST: refining text knowledge with optimal spatio-temporal descriptor for general video recognition. In *CVPR*, pages 18888–18898, 2024. [3](#), [5](#), [6](#), [7](#)
- [7] DeepSeek-AI. Deepseek-v2: A strong, economical, and efficient mixture-of-experts language model. *arXiv preprint arXiv:2405.04434*, 2024. [2](#), [5](#)
- [8] Jacob Devlin, Ming-Wei Chang, Kenton Lee, and Kristina Toutanova. BERT: pre-training of deep bidirectional transformers for language understanding. In *NAACL*, pages 4171–4186, 2019. [3](#)
- [9] Jian Ding, Nan Xue, Gui-Song Xia, and Dengxin Dai. Decoupling zero-shot semantic segmentation. In *CVPR*, pages 11573–11582, 2022. [3](#)
- [10] Alexey Dosovitskiy, Lucas Beyer, Alexander Kolesnikov, Dirk Weissenborn, Xiaohua Zhai, Thomas Unterthiner, Mostafa Dehghani, Matthias Minderer, Georg Heigold, Sylvain Gelly, Jakob Uszkoreit, and Neil Houlsby. An image is worth 16x16 words: Transformers for image recognition at scale. In *ICLR*, 2021. [3](#)
- [11] Deniz Engin and Yannis Avrithis. Zero-shot and few-shot video question answering with multi-modal prompts. In *ICCV Workshops*, pages 2797–2802, 2023. [3](#)
- [12] Chengjian Feng, Yujie Zhong, Zequn Jie, Xiangxiang Chu, Haibing Ren, Xiaolin Wei, Weidi Xie, and Lin Ma. Promptdet: Towards open-vocabulary detection using uncurated images. In *ECCV*, pages 701–717, 2022. [1](#)
- [13] Raghav Goyal, Samira Ebrahimi Kahou, Vincent Michalski, Joanna Materzynska, Susanne Westphal, Heuna Kim, Valentin Haenel, Ingo Fründ, Peter Yianilos, Moritz Mueller-Freitag, Florian Hoppe, Christian Thureau, Ingo Bax, and Roland Memisevic. The “something something” video database for learning and evaluating visual common sense. In *ICCV*, pages 5843–5851, 2017. [2](#), [5](#), [6](#)
- [14] Kaiming He, Xiangyu Zhang, Shaoqing Ren, and Jian Sun. Delving deep into rectifiers: Surpassing human-level performance on imagenet classification. In *ICCV*, pages 1026–1034, 2015. [5](#)
- [15] Fabian Caba Heilbron, Victor Escorcia, Bernard Ghanem, and Juan Carlos Niebles. Activitynet: A large-scale video benchmark for human activity understanding. In *CVPR*, pages 961–970, 2015. [2](#)
- [16] Neil Houlsby, Andrei Giurgiu, Stanislaw Jastrzebski, Bruna Morrone, Quentin de Laroussilhe, Andrea Gesmundo, Mona Attariyan, and Sylvain Gelly. Parameter-efficient transfer learning for NLP. In *ICML*, pages 2790–2799, 2019. [4](#), [7](#)
- [17] Edward J. Hu, Yelong Shen, Phillip Wallis, Zeyuan Allen-Zhu, Yuanzhi Li, Shean Wang, Lu Wang, and Weizhu Chen. Lora: Low-rank adaptation of large language models. In *ICLR*, 2022. [2](#), [4](#), [7](#)
- [18] Chen Ju, Tengda Han, Kunhao Zheng, Ya Zhang, and Weidi Xie. Prompting visual-language models for efficient video understanding. In *ECCV*, pages 105–124, 2022. [6](#), [7](#)
- [19] Muhammad Uzair Khattak, Hanoona Abdul Rasheed, Muhammad Maaz, Salman H. Khan, and Fahad Shahbaz Khan. Maple: Multi-modal prompt learning. In *CVPR*, pages 19113–19122, 2023. [1](#), [3](#)
- [20] Hildegard Kuehne, Hueihan Jhuang, Estíbaliz Garrote, Tomaso A. Poggio, and Thomas Serre. HMDB: A large video database for human motion recognition. In *ICCV*, pages 2556–2563, 2011. [2](#), [5](#), [6](#)
- [21] Junnan Li, Dongxu Li, Silvio Savarese, and Steven C. H. Hoi. BLIP-2: bootstrapping language-image pre-training with frozen image encoders and large language models. In *ICML*, pages 19730–19742, 2023. [1](#), [2](#)
- [22] Ilya Loshchilov and Frank Hutter. Decoupled weight decay regularization. In *ICLR*, 2019. [5](#)
- [23] Timo Lüddecke and Alexander S. Ecker. Image segmentation using text and image prompts. In *CVPR*, pages 7076–7086, 2022. [1](#)
- [24] Bolin Ni, Houwen Peng, Minghao Chen, Songyang Zhang, Gaofeng Meng, Jianlong Fu, Shiming Xiang, and Haibin Ling. Expanding language-image pretrained models for general video recognition. In *ECCV*, pages 1–18, 2022. [2](#), [3](#), [5](#), [6](#), [7](#)
- [25] Junting Pan, Ziyi Lin, Xiatian Zhu, Jing Shao, and Hongsheng Li. St-adapter: Parameter-efficient image-to-video transfer learning. In *NeurIPS*, 2022. [2](#)
- [26] Zhiliang Peng, Wenhui Wang, Li Dong, Yaru Hao, Shaohan Huang, Shuming Ma, and Furu Wei. Kosmos-2: Grounding multimodal large language models to the world. *arXiv preprint arXiv:2306.14824*, 2023. [2](#)
- [27] Yijun Qian, Lijun Yu, Wenhe Liu, and Alexander G. Hauptmann. Rethinking zero-shot action recognition: Learning from latent atomic actions. In *ECCV*, pages 104–120, 2022. [6](#), [7](#)
- [28] Alec Radford, Jong Wook Kim, Chris Hallacy, Aditya Ramesh, Gabriel Goh, Sandhini Agarwal, Girish Sastry, Amanda Askell, Pamela Mishkin, Jack Clark, Gretchen Krueger, and Ilya Sutskever. Learning transferable visual models from natural language supervision. In *ICML*, pages 8748–8763, 2021. [1](#), [2](#), [3](#)
- [29] Hanoona Abdul Rasheed, Muhammad Uzair Khattak, Muhammad Maaz, Salman H. Khan, and Fahad Shahbaz Khan. Fine-tuned CLIP models are efficient video learners. In *CVPR*, pages 6545–6554, 2023. [1](#), [3](#), [6](#)

- [30] Shuvendu Roy and Ali Etemad. Consistency-guided prompt learning for vision-language models. In *ICLR*, 2024. 2
- [31] Khurram Soomro, Amir Roshan Zamir, and Mubarak Shah. UCF101: A dataset of 101 human actions classes from videos in the wild. *arXiv preprint arXiv:1212.0402*, 2012. 2, 5, 6
- [32] Zhan Tong, Yibing Song, Jue Wang, and Limin Wang. Video-mae: Masked autoencoders are data-efficient learners for self-supervised video pre-training. In *NeurIPS*, 2022. 6
- [33] Aäron van den Oord, Yazhe Li, and Oriol Vinyals. Representation learning with contrastive predictive coding. *arXiv preprint arXiv:1807.03748*, 2018. 2
- [34] Mengmeng Wang, Jiazheng Xing, and Yong Liu. Actionclip: A new paradigm for video action recognition. *arXiv preprint arXiv:2109.08472*, 2021. 2, 3, 7
- [35] Yi Wang, Kunchang Li, Yizhuo Li, Yinan He, Bingkun Huang, Zhiyu Zhao, Hongjie Zhang, Jilan Xu, Yi Liu, Zun Wang, Sen Xing, Guo Chen, Junting Pan, Jiashuo Yu, Yali Wang, Limin Wang, and Yu Qiao. Internvideo: General video foundation models via generative and discriminative learning. *arXiv preprint arXiv:2212.03191*, 2022. 2
- [36] Yi Wang, Yinan He, Yizhuo Li, Kunchang Li, Jiashuo Yu, Xin Ma, Xinhao Li, Guo Chen, Xinyuan Chen, Yaohui Wang, Ping Luo, Ziwei Liu, Yali Wang, Limin Wang, and Yu Qiao. Internvid: A large-scale video-text dataset for multimodal understanding and generation. In *ICLR*, 2024. 1, 2, 3, 5
- [37] Syed Talal Wasim, Muzammal Naseer, Salman H. Khan, Fahad Shahbaz Khan, and Mubarak Shah. Vita-clip: Video and text adaptive CLIP via multimodal prompting. In *CVPR*, pages 23034–23044, 2023. 2, 3, 6, 7
- [38] Zejia Weng, Xitong Yang, Ang Li, Zuxuan Wu, and Yu-Gang Jiang. Open-vclip: Transforming CLIP to an open-vocabulary video model via interpolated weight optimization. In *ICML*, pages 36978–36989, 2023. 3
- [39] Xiaoshi Wu, Feng Zhu, Rui Zhao, and Hongsheng Li. CORA: adapting CLIP for open-vocabulary detection with region prompting and anchor pre-matching. In *CVPR*, pages 7031–7040. 1
- [40] Lingxiao Yang, Ru-Yuan Zhang, Yanchen Wang, and Xiaohua Xie. MMA: multi-modal adapter for vision-language models. In *CVPR*, pages 23826–23837, 2024. 2
- [41] Taojiannan Yang, Yi Zhu, Yusheng Xie, Aston Zhang, Chen Chen, and Mu Li. AIM: adapting image models for efficient video action recognition. In *ICLR*, 2023. 2
- [42] Lu Yuan, Dongdong Chen, Yi-Ling Chen, Noel Codella, Xiyang Dai, Jianfeng Gao, Houdong Hu, Xuedong Huang, Boxin Li, Chunyuan Li, Ce Liu, Mengchen Liu, Zicheng Liu, Yumao Lu, Yu Shi, Lijuan Wang, Jianfeng Wang, Bin Xiao, Zhen Xiao, Jianwei Yang, Michael Zeng, Luowei Zhou, and Pengchuan Zhang. Florence: A new foundation model for computer vision. *arXiv preprint arXiv:2111.11432*, 2021. 2
- [43] Renrui Zhang, Wei Zhang, Rongyao Fang, Peng Gao, Kunchang Li, Jifeng Dai, Yu Qiao, and Hongsheng Li. Tip-adapter: Training-free adaption of clip for few-shot classification. In *ECCV*, pages 493–510, 2022. 1, 3
- [44] Minghao Zhu, Zhengpu Wang, Mengxian Hu, Ronghao Dang, Xiao Lin, Xun Zhou, Chengju Liu, and Qijun Chen. Mote: Reconciling generalization with specialization for

visual-language to video knowledge transfer. *arXiv preprint arXiv:2410.10589*, 2024. 2, 3, 6, 7